Within Host Evolution Results in Antigenically Distinct GII.4 Noroviruses

Kari Debbink[a], Lisa C. Lindesmith[b], Martin T. Ferris[c], Jesica Swanstom[b], Martina Beltramello[d], Davide Corti[d,e], Antonio Lanzavecchia[d,f], and Ralph S. Baric[a,b]#

Department of Microbiology and Immunology, University of North Carolina, Chapel Hill, NC, USA[a]; Department of Epidemiology, University of North Carolina, Chapel Hill, NC, USA[b]; Department of Genetics, University of North Carolina, Chapel Hill, NC, USA[c]; Institute for Research in Biomedicine, Bellinzona, Switzerland[d]; Humabs Biomed SA, Bellinzona, Switzerland[e]; Institute of Microbiology, ETH Zurich, Zurich, Switzerland[f]

Running Head: Norovirus Within Host Evolution

#Address correspondence to Ralph Baric, rbaric@sph.unc.edu

Abstract word count: 193

Text word count: 5,663

Abstract

GII.4 noroviruses are known to rapidly evolve, with the emergence of a new primary strain every 2-4 years as herd immunity to the previously-circulating strain is overcome. Because viral genetic diversity is higher in chronic as compared to acute infection, chronically-infected immunocompromised people have been hypothesized as a potential source for new epidemic GII.4 strains. However, while some capsid protein residues are under positive selection and undergo patterned changes in sequence variation over time, the relationships between genetic variation and antigenic variation remains unknown. Based on previously-published GII.4 strains from a chronically-infected individual, we synthetically reconstructed VLPs representing an early and late isolates from a small bowel transplant patient chronically infected with norovirus, as well as the parental GII.4-2006b strain. We demonstrate that intra-host GII.4 evolution results in the emergence of antigenically distinct strains over time, comparable to the variation noted between chronologically predominant GII.4 strains GII.4-2006b and GII.4-2009. Our data suggest that in some individuals the evolution that occurs during a chronic norovirus infection overlaps with changing antigenic epitopes that are associated with successive outbreak strains and may select for isolates that are potentially able to escape herd immunity from earlier isolates.

Importance

Noroviruses are agents of gastrointestinal illness, infecting an estimated 21 million people per year in the United States alone. In healthy individuals, symptomatic infection typically resolves within 24-48 hours. However, symptoms

may persist years in immunocompromised individuals, and development of successful treatments for these patients is a continued challenge. This work is relevant to the design of successful norovirus therapeutics for chronically infected patients, provides support for previous assertions that chronically infected individuals may serve as reservoirs for new, antigenically unique emergent strains, and furthers our understanding of GII.4 norovirus immune-driven molecular evolution.

Introduction

Noroviruses are the leading cause of gastrointestinal illness worldwide. While typically an acute disease, norovirus infections can be serious in the young, old, and immunocompromised, as these groups are at risk for more severe disease and death (1-3). Norovirus is spread rapidly in environments where people are found in close proximity including schools and daycares, nursing homes, cruise ships, and hospitals. Importantly, hospital outbreaks can result in significant economic damage, with direct and indirect costs from a single outbreak reaching $650,000 (4).

Noroviruses are members of the Caliciviridae family and contain a ~7.5 kb single stranded, positive polarity RNA genome. They are divided into 5 genogroups; genogroups I and II are responsible for the majority of human disease and are further subdivided into at least 9 and 22 genotypes, respectively (5). The human norovirus genome encodes three open reading frames: the non-structural proteins, the ORF2 major capsid protein (VP1), and the ORF3 minor capsid protein (VP2) (6). VP1 is further divided into the shell (S) and protruding (P) domains, with the P domain is comprised of the P1 and P2 subdomains (6). Phylogenetic studies indicate that the P2 subdomain is the most variable region of the norovirus genome (7, 8). The P2 subdomain is also the most surface exposed region of the norovirus capsid, interacting with antibodies and histoblood group antigens, which serve as binding ligands and putative receptors for human norovirus docking and entry.

GII.4 strains cause over 70% of all norovirus outbreaks (9) and epidemic outbreaks occur every 2-4 years involving a new antigenically distinct strain (7, 10). Studies of antigenic variation in GII.4 norovirus have shown that the P2 region is involved in strain specific antibody recognition (7, 11, 12), and contains at least three blockade (potential neutralization) epitopes (13-15). In epidemic strains, genetic variation in P2 is linked to antigenic changes over time, indicating that molecular evolution in the P2 subdomain is likely driven by escape from human herd immunity (12-17).

Noroviruses typically cause acute infection in healthy individuals, resulting in symptomatic infection for 24-48 hours followed by viral shedding for two to four weeks (18, 19). However, some immunocompromised individuals such as transplant patients on immunosuppressive drugs, those with primary immunodeficiencies, cancer patients undergoing chemotherapy, and those with HIV may develop chronic norovirus infection. Symptomatic infection and viral shedding in these patients can persist from weeks to years (20-25) and can result in medical issues such as dehydration and nutrient deficiencies (26), making development of treatment options for these patients an important priority. Unfortunately, there are no approved therapeutics or vaccines for controlling norovirus infections. Attempted methods to control chronic infection have included treatment with drugs effective against other diarrheal diseases (27), adjustment of immunosuppressive drug type or dosage (28), and oral or enteral administration of human IgG (29-32). Although reduction in immunosuppression coupled with IgG administration has shown promise for some transplant patients,

IgG therapy has failed in other studies, and reduction of immunosuppression is not always possible.

Existing studies provide a basis to investigate important questions about chronic norovirus infection. Although unconfirmed, one recent hypothesis is that chronically infected norovirus patients may be important sources of infection both in healthcare settings (33) and as potential reservoirs for new emergent GII.4 norovirus strains (20, 23, 25). Although the fitness and the infectivity of chronically shed virus is currently unknown, potential accounts of chronic norovirus shedders involved in hospital outbreaks and transmission of virus to both immunocompromised and immunocompetent individuals have been documented (21, 33, 34).

Virus capsid sequence and phylogenetic data from chronically infected patients have found substantial genetic variation over the course of infection in many, but not all, patients (22, 23, 35). Siebenga et al. found that capsid mutation rate was linked to immune impairment, suggesting that immune-driven selection drives evolution in the capsid during chronic infection (35), and explains differences in evolution depending on level of immunosuppression. Additional studies have corroborated a role for intra-host immune driven selection by demonstrating that virus isolated from chronically-infected patients undergoes positive selection and exhibits higher genetic diversity in the capsid protein than virus from acutely infected individuals (23, 25). In some chronically infected patients with GII.4 strain infections, many of the changes occur in blockade

117 epitopes, areas of known or predicted antigenic importance but antigenic
118 comparisons have not been performed (13-15, 22, 35).
119 In this manuscript, we compare and contrast the antigenic differences
120 using a panel of polyclonal and monoclonal antibodies and time-ordered VLPs
121 derived from early (day 1—P.D1) and late (day 302—P.D302) capsid protein
122 amino acid sequences from a chronically infected immunocompromised patient
123 (23). Our data demonstrate significant antigenic differences between intra-host
124 variants that mirrors the degree of variation seen in major successive norovirus
125 strains, suggesting that chronic norovirus infections can evolve antigenically
126 unique variants with the potential to seed future norovirus outbreaks.
127

Methods

Sequences and Structural Homology Models

GenBank (NCBI sequence database) sequences used in this study were JQ478409.1 (GII.4-2006b) (15), JQ417309 (P_04.2009 or P.D1) (23), JQ417327 (P_02.2010 or P.D302) (23), JN595867.1 (GII.4-2009) (15), and JX459908.1 (GII.4-2012) (36), and the VA387 crystal structure is available from the RCSB Protein Data Bank: identifier 2OBT (37). We refer to originally-named P_04.2009 as P.D1 and P_02.2010 as P.D302 for simplicity throughout the manuscript. Homology models of these sequences were constructed using Modeller (Max-Planck Institutue for Developmental Biology) and modeled in PyMOL.

Production of VRPs. Virus replicon particles (VRPs) encoding the norovirus major capsid gene were produced as previously described (38). Briefly, expression vector pVR21 encodes the VEE genome with the VEE structural genes replaced with a commercially synthesized norovirus ORF2 gene (BioBasic) behind the 26S promoter. The VEE-norovirus ORF2 construct and two separate plasmids expressing either the VEE 3526 E1 and E2 glycoproteins or VEE 3526 capsid protein were used to make RNA. RNA from all three constructs was electroporated into BHK cells, and 48 hours later VRPs were harvested and purified by high speed centrifugation. VRP titers were determined by counting fluorescent cells detected with FITC-labeled antibody. VLP production from VRPs and structural integrity was confirmed by EM.

151 **Production of VLPs.** VLPs were produced as previously described (13, 15).
152 Briefly, commercially synthesized norovirus ORF2 (BioBasic) from chronically
153 infected patient sequence or outbreak strain sequence was cloned into
154 expression vector pVR21 behind the 26S promotor, and genome length RNAs
155 were synthesized in vitro using T7 RNA polymerase. RNA from the VEE-ORF2
156 construct and helper RNAs was electroporated into BHK cells, and 24 hours later
157 VLPs were harvested and purified by high speed centrifugation. VLP
158 concentration was determined by BCA Protein Assay (Pierce), and structural
159 integrity was confirmed for all VLPs by EM.
160
161 **HBGA Binding Assay.** HBGA assays were performed as previously described
162 (7). Briefly, Avidin coated plates (Pierce) were coated with 10 ug/mL synthetic
163 biotinylated HBGAs (GlycoTech), followed by addition of 2 ug/mL VLPs. HBGA
164 binding was detected by strain specific mouse polyclonal sera followed by anti-
165 mouse IgG-HRP (GE Healthcare) and then One-Step Ultra TMB HRP substrate.
166 Positive reactivity for each HBGA is defined as an OD 450 nm signal above or
167 equal to 3X the background binding (background range 0.049-0.066) after
168 background subtraction.
169
170 **EIAs.** Reactivity with mouse and human mAbs was determined by enzyme-linked
171 immunoassay (EIA). Plates were coated with 0.5 µg/ml VLP in PBS, and then
172 two-fold serial dilutions of mAb starting at 1 µg/ml mAb were added. Anti-mouse
173 or human IgG-HRP (GE Healthcare) followed by One-Step Ultra TMB EIA HRP

substrate solution was used for detection. Positive reactivity is defined as a mean OD 450 nm $\geq$0.2 after background subtraction. Data represent the combination of three independent trials with each VLP run in duplicate in each trial. Sigmoidal dose response analysis was performed as previously described (14) using the reactivity at 1 ug/ml as 100% binding. EC_{50} values among VLPs were compared using One-way ANOVA with Dunnett's post test. $P<0.05$ was considered significant. VLPs with maximum reactivity below mean OD 450 nm 0.2 were assigned a value of zero for graphical representations.

VLP-Carbohydrate Ligand-Binding Antibody Blockade Assays.

Blockade assays using Pig Gastric Mucin Type III (Sigma Chemicals) were performed as previously described (14). PGM-bound VLPs were detected by rabbit anti-GII.4 norovirus polyclonal sera. The percent control binding was defined as the VLP-ligand binding level in the presence of test antibody or sera compared to the binding level in the absence of antibody multiplied by 100. All mAbs and sera were tested for blockade potential at two-fold serial dilutions ranging from 0.0039 to 2 µg/ml (mouse mAbs), 0.0039 to 16 µg/ml (human mAbs), and 0.0098 to 5% (mouse sera). Data from blockade experiments using monoclonal antibodies represent the combination of three independent trials with each VLP run in duplicate in each trial. Data from blockade experiments using polyclonal mouse sera represent the combination of two independent trials in which sera from five individual mice were tested for each VLP. Sigmoidal dose response analysis was performed as previously described, and EC_{50} values

among VLPs were compared using One-way ANOVA with Bonferroni post test. $P<0.05$ was considered significant. Blockade assays utilize VLP concentrations in the low nanomolar range; therefore, this assay does not discriminate between antibodies with sub-nanomolar affinities.

Monoclonal antibodies and mouse polyclonal sera

Mouse (12) and human (14) monoclonal antibodies were isolated as previously described. Balb/c mice (five per group) were immunized by footpad injection with 5×10^4 VRPs expressing norovirus capsid gene (GII.4-1987, GII.4-2002, GII.4-2006b, GII.4-2009, P.D1, or P.D302). Mice were boosted on day 21, euthanized 7 days post-boost, and sera were harvested. This study followed all institutional guidelines for animal care and experimentation (IACUC guidelines).

Antigenic Cartography

We utilized multi-dimensional scaling (MDS) approaches as described and implemented within the AntigenMap 3D software (39, 40). The EC_{50} blockade titers of various sera against a panel of VLPs were normalized to maximum blockade titer of each sera, as well as to the maximum overall blockade titer across sera (Normalization method 1 in AntigenMap 3D). Normalized values were used to calculate Euclidean distances, D, between each pair of VLPs. For greater analytic, visualization, and graphical purposes, we then utilized Matlab8.1's (MathWorks Inc, Natick, MA) cmdscale function to determine the XYZ coordinates such that the data can be displayed in 3 dimensions while

maintaining the underlying Euclidean distances directly calculated from the data. We utilized R (www.r-project.org), with the package rgl for 3D visualization of these data. We confirmed the output of our pipeline with that produced by AntigenMap 3D.

Results

Comparison of sequence changes among chronic infection isolates GII.4-2006b.

Previous work has shown that changes identified in a few key surface exposed epitopes correlate with shifts in GII.4 norovirus antigenicity (11, 13-15), including residues in Epitope A (294, 296-298, 368, and 372) (13), Epitope D (393-395) (14), and Epitope E (407, 412-413) (15). Changes in these residues likely alter the ability of preexisting immunity to neutralize the virus, selecting for the emergence of new epidemic strains.

To study the within-host antigenic evolution of noroviruses during a chronic human infection, we aligned the sequence of the capsid P2 domains of GII.4-2006b, P.D1, and P.D302 to examine sequential amino acid changes from GII.4-2006b through P.D302 after at least 10 months of within-host evolution (23). Note that day 1 and day 302 refer to the days of sample collection and not from beginning of infection, as the time between the beginning of infection and the collection of the day 1 sample is unknown. Between VP1 amino acid positions 248-434, there are 9 differences between GII.4-2006b and P.D1. After 10 months, there were 15 additional differences between P.D1 and P.D302, and 20 differences between GII.4-2006b and P.D302 located between these amino acid positions (Figure 1A). Similarly, there are 16 differences spanning this domain between GII.4-2006b and subsequent epidemic strains, GII.4-2009 and GII.4-2012. Two of the differences between GII.4-2006b and P.D1 (S368A and S393G) and four of the differences between GII.4-2006b and P.D302 (A294G,

S296T, S368A, and N412D) are located within blockade epitope sites (Figure 1B). Four differences in blockade epitope residues also exist between P.D1 and P.D302 (A294G, S296T, G393S, N412D) (Figure 1B). We synthesized GII.4-2006b, P.D1, and P.D302 genes, expressed VLPs representing these strains, and measured differences in antigenicity and HBGA binding among the chronic infection isolates and GII.4-2006b using biological assays. In addition, several amino acid substitutions present in the chronic infection strains that are conserved in past epidemic strains may also influence the antigenic and HBGA binding characteristics of epitope sites A (292, 295, 373), D (391), and E (414) (Figure 1B) based on their position relative to these epitopes in GII.4 homology models (Figure 1C).

Comparison of HBGA binding in chronic infection isolates to GII.4-2006b.

To evaluate differences in HBGA binding preferences among GII.4-2006b, P.D1, and P.D302, we measured VLP binding to synthetic biotinylated carbohydrates (A, B, Le^a, Le^b, Le^x, Le^y, H type 1, and H type 3). As previously reported, GII.4-2006b bound A, B, Le^b, Le^y, and H type 3 (41). In contrast, chronic infection strain VLPs exhibited differential HBGA binding profiles compared to GII.4-2006b and to each other (Table 1). P.D1 was able to bind A, B, and H type 3, while P.D302 bound only B and H type 3 synthetic biotinylated HBGAs. This indicates that HBGA binding preferences may be altered over time during chronic infection, perhaps influenced by individual within host HBGA expression phenotypes.

Reactivity with GII.4 Mouse and Human mAbs

To measure antigenic differences among VLPs representing GII.4-2006b and chronic strains P.D1 and P.D302, we performed enzyme-linked immunoassays (EIAs) using mouse and human mAbs. We tested five GII.4-2006b mouse mAbs (G2, G3, G4, G6, G7) and two GII.4 human mAbs (NVB111, NVB43.9), all of which target epitope site A residues (294, 296-298, 368, and 372), for EIA binding with GII.4-2006b, P.D1, and P.D302 VLPs. GII.4-2006b and P.D1 differ in one epitope site A position, where P.D1 contains S368A compared to GII.4-2006b. P.D302 is different from GII.4-2006b at 3/6 epitope site A residues: A294G, S296T, and S368A, while P.D1 and P.D302 are different at 2/6 epitope site A residues: A294G and S296T. We also tested reactivity of these VLPs with one human mAb (NVB97), which targets epitope site D residues (393-395). While GII.4-2006b and P.D302 share identical epitope site D residues, P.D1 has an S393G change compared to GII.4-2006b. We additionally tested one human mAb (NVB71.4) that targets an unmapped conserved GII.4 epitope (14). Consistent with previously-reported results, all mAbs reacted strongly with GII.4-2006b VLPs (12, 14) (Table 2). In contrast, EC_{50} values for P.D1 VLPs were significantly different ($P<0.05$) from GII.4-2006b VLPs for mouse mAbs G2, G4, G6, and human mAbs NVB43.9, and NVB111 (Table 2). Moreover, EC_{50} values for P.D302 VLPs were significantly different from GII.4-2006b for all mAbs except NVB71.4, and different from P.D1 VLPs for all but NVB71.4 and NVB111 (Table 2). This indicates that epitope sites A and D are antigenically distinct

among GII.4-2006b, P.D1, and P.D302, demonstrating antigenic variation over the course of chronic infection in important blockade epitopes.

Blockade Activity for GII.4 Mouse and Human mAbs

Compared to EIA, neutralization is a more relevant measure of functional antigenic change. To test potential neutralization activity of mAbs (GII.4-2006b-G2, G3, G4, G6, and G7, and NVB43.9, NVB71.4, NVB97, NVB111) against GII.4-2006b, P.D1, and P.D302 VLPs, we performed blockade assays, a correlate of protective immunity (42) and a neutralization surrogate. Consistent with previous findings, all mAbs were able to block ligand-VLP interactions for GII.4-2006b (12, 14) (Figure 2). Likewise, P.D1 was blocked by all mAbs (Figure 2). However, EC_{50} blockade titers for two out of five GII.4-2006b mouse mAbs, G2 (Figure 2A) and G7 (Figure 2E), and two of four GII.4 human mAbs, NVB111 (Figure 2G) and NVB71.4 (Figure 2I), were significantly different, requiring 7.1X, 2X, 2X, 3.2X more antibody, respectively, for blockade compared to GII.4-2006b VLPs. P.D302 VLP-ligand binding was blocked by GII.4-2006b mouse mAbs G2 (Figure 2A), G6 (Figure 2D), G7 (Figure 2E), but not by G3 (Figure 2B) or G4 (Figure 2C), and blocked by GII.4 human mAb NVB71.4 (Figures 2I), but not by NVB43.9 (Figure 2F), NVB111 (Figure 2G), or NVB97 (Figures 2H). EC_{50} blockade titers were significantly different between GII.4-2006b and P.D302 for G2, G6, G7, and NVB71.4, requiring 12.6X, 15.9X, 12X, and 6.8X more mAb compared to GII.4-2006b, respectively. Overall, EC_{50} blockade titers were significantly higher for P.D302 compared to both GII.4-2006 and P.D1 for all

315 tested mAbs, demonstrating major antigenic changes in epitope sites A and D
316 over the course of chronic norovirus infection.
317
318 **Blockade Response of Strain Specific Mouse Polyclonal Sera**
319 While monoclonal antibodies are informative of the changes in a single
320 epitope, polyclonal sera are needed to evaluate global antigenic changes. To
321 measure differences in the total antibody response, we immunized mice with
322 virus replicon particles (VRPs) expressing the capsid gene from GII.4-2006b,
323 P.D1, and P.D302 or GII.4-2009, the consecutive outbreak strain following GII.4-
324 2006, and measured the induced serum blockade responses (Figure 3). Mice
325 immunized with GII.4-2006b VRPs mounted a robust blockade response against
326 homotypic GII.4-2006b VLPs, while significantly more sera was needed to block
327 GII.4-2009, P.D1, and P.D302 VLPs (16X, 9.4X, and 12.7X, respectively) (Figure
328 3A). Sera from mice immunized with GII.4-2009 VRPs induced a strong
329 blockade response against GII.4-2009 VLPs; however, significantly more sera
330 was needed to block GII.4-2006b and P.D302 VLPs, with 39X more sera needed
331 to block P.D302 VLPs compared to GII.4-2009 (Figure 3B). Sera from mice
332 immunized with P.D1 VRPs most efficiently blocked homotypic P.D1 VLPs. EC_{50}
333 values indicated that more sera is required to block GII.4-2009 (3X) and P.D302
334 (25.8X) than P.D1, while GII.4-2006b and P.D1 EC_{50} titers were not significantly
335 different (Figure 3C). Sera from mice immunized with P.D302 VRPs efficiently
336 blocked P.D302 VLP-ligand interactions and weakly blocked GII.4-2006b and
337 P.D1, requiring 92X and 61X more sera, respectively. P.D302 sera was unable

to block GII.4-2009 VLPs (Figure 3D). This data shows that chronic isolate VLPs induce antibody responses that are different from the parental strain and each other, demonstrating major changes in total antibody response over the course of chronic infection.

Antigenic Cartography

In order to further describe and visualize the differences between virus strains in their antigenic properties, we utilized the multi-dimensional scaling (MDS) approach known as antigenic cartography (39,40). Specifically, we used the pipeline described in AntigenMap 3D (39) to measure and visualize the antigenic relationships among outbreak strains GII.4-1987, GII.4-1997, GII.4-2002, GII.4-2006b, GII.4-2009, and GII.4-2012 as well as chronic isolates P.D1 and P.D302, explicitly contrasting antigenic relationships between naturally occurring epidemic strains as well as intra-host variants. The antigenic distances between strains were measured using GII.4-1987, GII.4-2002, GII.4-2006b, GII.4-2009, P.D1, and P.D302 mouse sera EC_{50} blocking titers against VLPs representative of the specified GII.4 strains, and Euclidean distance values were calculated based on these titers (Figure 4A). Consistent with earlier findings (12), early (GII.4-1987, GII.4-1997, GII.4-2002) and late strains (GII.4-2006b, GII.4-2009, GII.4-2012) formed distinct clusters (Figure 4B-C). Not surprisingly, the early within host variant, P.D1, grouped closely with late strains (Figure 4B-C), reflecting its origins from the GII.4-2006b lineage. In contrast, P.D302 did not group with any other strain and was antigenically distant from both the early and

contemporary isolates. In order to confirm the visual analysis of these antigenic similarities, we compared Euclidean distances, D, between each pair of VLPs across all serum utilized for antigenic cartography (the Euclidean distance measures the straight-line distance between two points in a multidimensional space). We first examined the groupings of early and late GII.4 outbreak strains. The average distance within a group was 3.79 (range 2.11-6.39) while the average distance between early and contemporary clusters was 10.7 (range 8.49-13.32), with each distance unit corresponding to a roughly 1.25-fold difference in blockade response between viruses (Figure 4A). As shown in Figures 4B and 4C, P.D1 grouped closely with late outbreak strain VLPs, with an average D of 3.46 (range 2.26-5.09) (Figure 4A). In contrast, P.D302 was quite distinct from both early and late outbreak strain viruses, as well as from P.D1, with an average D of 9.92 (range 8.73-11.62) (Figure 4A). During an ~10 month chronic infection in this individual, our data demonstrate that intra-host evolution can generate novel variants with unique HBGA binding patterns and encode unique antigenic differences that are as dramatically distinct as time-ordered, epidemic outbreak strains that emerge in human populations.

Expansion of Epitope Site A

We next determined whether novel sites of within host evolution can refine existing epitope maps and identify potential immunogenic changes in epidemic strains of the future. Amino acid position 373 exhibited a N373H change between P.D1 and P.D302 but was conserved in major GII.4 epidemic strains up until a

N373R substitution emerged in GII.4-2012 Sydney. Although not supported with empirical data, recent work by Allen et al (43) suggests that this change in the Sydney strain may have impacted its emergence. Since changes to 373 have never been shown to influence immunogenicity, and it is not included as a diagnostic A epitope site residue, this potentially hampers new epidemic strain identification. To determine whether position 373 contributes to antigenic differences in epitope A, we used the blockade assay to test potential neutralization of VLPs representing parental strains GII.4-2009 New Orleans, GII.4-2012 Sydney, and chimeric sequences GII.4-2012.09A, GII.4-2012.09A.R373N, and GII.4-2012.R373N (Figure 5) by epitope A targeting human mAb 43.9. GII.4-2009 was efficiently blocked by mAb 43.9, while GII.4-2012 required significantly more (55.3X) mAb for blockade. Blockade response was partially restored in chimeras GII.4-2012.09A and GII.4-2012.R373N, but required 1.5X and 4.8X more mAb, respectively, for blockade compared to GII.4-2009. EC_{50} blockade titers were not statically different between GII.4-2012.09A.R373N and GII.4-2009 VLPs. Similar trends were seems using mouse mAbs targeting epitope A residues (data not shown).

Discussion

Noroviruses are an important cause of gastroenteritis in immunocompromised individuals (44, 45), who are at increased risk for severe disease outcomes (1, 44). Recent vaccine trials utilizing a VLP-based vaccine approach support the idea that efficacious vaccines can be generated that elicit

short term protection in some healthy individuals, but vaccines may not protect immunocompromised populations, making development of therapeutics that effectively treat or prevent norovirus infections a top health priority.

In immunocompetent people, norovirus infection results in acute disease outcomes (46). In contrast, immunocompromised individuals can develop symptomatic disease and high titer viral shedding up to years. Unfortunately, the literature on specific chronically-infected norovirus patient populations is sparse, and duration and severity of chronic norovirus infections is likely influenced by several factors including underlying condition, drug treatment regime, degree of immunosuppression, and the rate of within host virus evolution, making it difficult to define the characteristics of a typical chronic norovirus case. From these limited studies, it is difficult to discern whether there are characteristics of chronic norovirus infection that are broadly applicable to all populations, characteristics that are true to specific populations, or whether characteristics vary by each individual case. Previous work has shown that during the course of chronic infection, virus genetic diversity can expand quickly (22, 23, 25, 35); however, it was previously unknown whether this genetic variation translated into antigenic variation or the emergence of antigenically unique isolates that differ significantly from contemporary epidemic strains. For the first time, our work clearly demonstrates the potential for significant antigenic variation over the course of chronic infection within an individual, which is important in terms of both therapeutic treatment considerations and for studying the potential role for chronic shedders as reservoirs for evolving new outbreak strains.

Since there is no known animal reservoir for human noroviruses (47), the available data indicate that new GII.4 strains likely arise naturally within the human population by epochal evolution, immune driven selection, and inter-host transmission over time (12-14, 16, 17). The occurrence of frequent long-term chronic infections in immunosuppressed patients also represents a possible source of new GII.4 norovirus strains with epidemic potential (23, 25, 35), as these patients may provide an appropriate environment for sustained immune-directed molecular evolution by targeting previously identified surface exposed blockade epitopes for mutation driven escape. Evidence supporting this hypothesis includes sequence data from chronically infected patients that demonstrate the emergence of genetic changes in GII.4 blockade epitopes that modulate inter-host antigenicity (22, 35). This diverse pool may contain variants antigenically distinct from the predominant circulating strain, allowing emergence of a new strain under the right conditions (25). However, host and environmental factors coupled with the type and degree of immunosuppression may affect the rate and complexity of intra-host evolution that occurs over time (23), and future work that evaluates the role of different immunosuppressive conditions on intra-host norovirus evolution are needed.

Our work demonstrated intra-host antigenic changes within epitope site A (amino acids 294, 296-298, 368, and 372). Interestingly, P.D302 contained residue substitutions in amino acid positions 292, 295, and 373, which are conserved in major GII.4 outbreak strains, except for 373, which was altered in the most recent predominant strain, GII.4-2012 Sydney. Changes in these

453 residues likely impact epitope A antibody binding and blockade response either
454 by altering the conformational landscape of the epitope or directly inhibiting the
455 interaction of the antibody with the capsid. Using GII.4-2009/GII.4-2012 chimeric
456 VLPs, we demonstrated that residues at position 373 impact the blockade
457 response of human mAb NVB 43.9, an antibody that targets epitope A. This
458 demonstrates that 373 is part of epitope A, expanding this epitope to 7 positions.
459 Furthermore, we suggest that monitoring intra-host evolved strains may provide a
460 novel diagnostic strategy to map key residues capable of mediating antigenic
461 changes in future outbreaks. While positions 292 and 295 have been conserved
462 in previous predominantly-circulating GII.4 strains, their ability to change in this
463 patient and their proximity to known epitope A residues suggest that these
464 residues could potentially impact antigenic change in epitope A in future
465 epidemics, as residue 373 did in GII.4-2012 Sydney.

466 Reactivity and blockade response data for antibody NVB97 demonstrates
467 antigenic evolution in epitope site D during chronic infection. Epitope site D
468 minimally include residues 393-395, is in close proximity to the carbohydrate
469 binding pocket (37), and previous work demonstrates that modulation of residues
470 within this epitope modulate HBGA specificity (7). Evolution in this epitope site is
471 likely driven both by antibody selective pressure and pressure to maintain binding
472 to one or more HBGAs. Despite conservation of residues 393-395 between
473 GII.4-2006b and P.D302, antigenic phenotypes differ significantly, demonstrating
474 that NVB97 recognition is modulated by amino acid positions outside of the
475 previously-defined epitope site D residues. Position 391, which is close to the

476 carbohydrate binding pocket, is conserved in major outbreak strains and between
477 GII.4-2006b and P.D1, and previous work demonstrated that an alanine
478 substitution at this residue had little impact on HBGA binding (48). Neither the
479 antigenic consequences of residue changes nor the impact of other residue
480 substitutions on HBGA binding at this position have been rigorously evaluated,
481 meaning that the D391N change in P.D302 may contribute to both the HBGA
482 reactivity and antibody blockade differences observed for P.D302. To explore
483 this possibility, we created homology models of these P2 domains and compared
484 the predicted polar interactions present in residues 390-395 (Figure 6) among
485 GII.4-2006b, P.D1, and P.D302.
486 Conformational comparisons between GII.4-2006b and P.D1 show
487 general similarities in the shape created by residues 390-395, with exceptions
488 being the loss of a side chain in 393 of P.D1, and slight shifts in position for side
489 chains in residues 394 and 395 (Figure 6A and 6B). These conformational
490 changes appear to impact the polar interactions within these residues, as the
491 loss of the side chain in residue 393 ablates the hydrogen bond present in GII.4-
492 2006b. In addition, the positional shifts in residues 394 and 395 in P.D1 appear
493 to prevent formation of another hydrogen bond present in GII.4-2006b.
494 Conformational comparisons between GII.4-2006b and P.D302 demonstrate that
495 the residue change at 391 has significant impact on the shape and hydrogen
496 bonding networks for residues 390-395 (Figures 6A and 6C). In P.D302, position
497 391 is bent downward, which differs from the position of this amino acid in GII.4-
498 2006b and P.D1. The result of this change is the formation of a hydrogen bond

between the side chain and main chain of 391. In addition, though residue 393 is conserved between GII.4-2006b and P.D302, the side chain is shifted downward in P.D302 compared to GII.4-2006b, shifting the position of the hydrogen bond found at this residue. The formation of two additional novel hydrogen bonds between 390 & 393 and 390 & 395 suggests that the 391 residue change and resulting conformational changes allowed for these increased polar interactions. A slight conformational shift in residue 395 in P.D302 appears to ablate a polar interaction found in GII.4-2006b at this position. We also compared polar interactions of GII.4-2006, P.D1, and P.D302 to residues outside of 390-395 (Figure 6D-F). GII.4-2006b and P.D1 displayed five conserved polar interactions to surrounding amino acids (Figures 6D and 6E), while P.D302 lost the polar interaction at residue 391 and gained an additional bond at residue 394 (Figure 6F).

In addition to epitope site D being an antibody blockade epitope, these residues modulate HBGA binding, so evolution in this region is likely driven both by antibody selective pressure and pressure to maintain binding to one or more HBGAs. Interestingly, all three structures maintained the two hydrogen bonds to positions 443 and 444. Residue 443 is in the HBGA binding site (37), and maintaining interaction with this residue may be selected for in this individual in order to retain HBGA binding. The altered HBGA binding profile and reduced NBV 97 binding and blockade for P.D302 may be explained by these polar differences, although this cannot be confirmed without a crystal structure of these P2 domains bound to NVB 97 and HBGAs.

522 Our demonstration of intra-host changes in HBGA binding profiles in a
523 chronically infected immunocompromised patient suggests that selection may
524 favor variants that bind patient-specific HBGAs. While speculative, the potential
525 emergence of intra-host variants that target patient-specific HBGA expression
526 profiles could select for the emergence of novel strains that recognize unique or
527 broad combinations of HBGA patterns, allowing for altered pathogenicity and
528 transmission efficiencies in an individual or across select human populations. We
529 could not evaluate this possibility in our study because the HBGA expression
530 profile of this chronically infected patient is unknown. Future research could
531 evaluate these HBGA phenotypic and FUT 2/3 genotypic relationships using
532 saliva and cells from chronically infected patients.
533 How much intra-host and inter-host antigenic variation is necessary to give
534 rise to a new strain that could escape herd immunity in the general population?
535 Using blockade EC_{50} data from mouse sera against GII.4-2006b, GII.4-2009
536 (representative of a successive outbreak strain), P.D1, and P.D302, we
537 demonstrate that the antigenic variation between P.D1 and P.D302 is 1.5X
538 greater than that seen between GII.4-2006b and GII.4-2009. To further address
539 this question, we used antigenic cartography, which provides easily interpretable
540 measures and visualization of multidimensional antigenic relationships, and has
541 previously been used to study antigenic differences in influenza strains (40, 49).
542 This analysis provided further support for the idea that within-host changes in the
543 virus can equal or exceed those differences seen across successive outbreak
544 strains, with the antigenic space between P.D302 and both GII.4-2006b (D=9.91)

and P.D1 (D=9.15) being greater than the average between the consecutive outbreak strains used in this study (average D=4.98; range 2.11 to 12.11) and mirrors the global difference between early GII.4 isolates (1987, 1997, 2002) and contemporary strains (2006b, 2009, 2012).

Antigenic cartography is a relatively new, powerful method with which to simply describe the multidimensional antigenic differences between virus strains. As such, there is room for improvement within these methods. Indeed, more complex statistical models underlying antigenic cartography approaches are being developed to better account for uncertainty within these datasets (49), and more comprehensive surveys of both antisera and natural GII.4 isolates over a 30-year time span will better allow for the characterization of antigenic change within noroviruses. Within this study, the use of mouse sera permits us to use an immunologically clean background with no pre-exposure history and provides a clearer starting point to evaluate specific relationships among outbreak strains and the intra-host isolates. Future work will require well defined, time-ordered human sera during natural epidemic outbreaks, time-ordered sera during intra-host chronic infections, and synthetic reconstruction of capsids representing both outbreak and unique panels of inter-host variants over time; unfortunately, to date, we have been unable to obtain the samples necessary to pursue this comprehensive investigation. Our data suggest that intra-host evolution over a 10-month period can yield sufficient antigenic change to escape existing herd immunity. Clearly, additional work examining norovirus infectivity after prolonged

567 shedding is needed in order to clarify whether chronically infected patients are a
568 probable source of novel epidemic strains.

569 Therapeutics are needed to alleviate clinical disease during long-term
570 norovirus infection and prevent the potential emergence of novel antigenic
571 variants with epidemic potential in the general population. Some success using
572 IgG to treat chronic norovirus (32) coupled with our data demonstrating that P.D1
573 is relatively antigenically similar to GII.4-2006b, while P.D302 is antigenically
574 divergent, suggest that treating early during chronic infection may be important
575 for viral clearance and also supports the possibility that similarly-administered
576 broadly neutralizing antibodies may be viable treatment options for patients
577 suffering from long-term norovirus infection. Our work demonstrates that GII.4
578 broadly-neutralizing mAb NVB71.4 retains blockade response against P.D1 and
579 P.D302, even though both these strains are antigenically distinct from GII.4-
580 2006b, GII.4-2009, and presumably other major GII.4 strains. This suggests that
581 NVB71.4 or other antibodies with broad cross-blockade activity could be isolated
582 and successfully used as norovirus therapeutics. Importantly, different
583 monoclonal antibodies will be needed that target other GI and GII strain chronic
584 infections. Furthermore, increased surveillance of norovirus isolates from
585 chronically infected patients as well as deep sequencing of patient isolates
586 should be considered in order to better understand the transmission dynamics
587 and genetic potential of norovirus isolates from these patients since these are
588 likely different from what is seen in the general population. Overall, our work
589 supports the idea that chronically infected individuals are potential reservoirs for

antigenically novel norovirus strains, and further work to characterize their role in transmission and emergent norovirus outbreaks and development of therapeutics to combat chronic infections should receive a top priority.

Acknowledgements

This work was supported by grant AI056351 from the National Institutes of Health, Allergy and Infectious Diseases and by institutional training grant T32-AI007419 from the National Institute of Health. The funders had no role in study design, data collection and analysis, decision to publish, or preparation of the manuscript. We thank Victoria Madden and C. Robert Bagnell, Jr., of the Microscopy Services Laboratory, Department of Pathology and Laboratory Medicine, University of North Carolina—Chapel Hill, for expert technical support. We also acknowledge the UNC-CH Genome Analysis Facility.

Figure Legends

Figure 1: Sequence Changes in Chronically Infected Patient Strains Compared to GII.4-2006b.

(A) Available capsid amino acid sequences for GII.4-2006b, P.D1 and P.D302 were aligned using Clustal Omega, and sequence differences among GII.4-2006, P.D1, and P.D302 are shown. GII.4-2006b residues are shown in purple. P.D1 and P.D302 differences from GII.4-2006b are indicated in light blue, while orange indicates a reversion to the GII.4-2006b residues. (B) Alignment of GII.4-2006b,

612 P.D1, and P.D302 amino acid sequences in and around Epitopes A, D, and E.
613 Green indicates a position within a defined epitope, while white indicates nearby
614 residues that may impact antigenicity in these epitopes. Yellow indicates an
615 amino acid position newly defined as part of epitope A. (C) Structural homology
616 models of GII.4-2006b, P.D1, and P.D302 capsid P2 dimers shown from top
617 view. Purple shows location of Epitopes A, D, and E on the capsid P2 dimer,
618 while green shows changing amino acid residues in P.D1 and P.D302 compared
619 to GII.4-2006b.

620

621 **Table 1: Chronic Infection Strain HBGA Binding Preferences**
622 VLPs representing GII.4-2006b, P.D1, and P.D302 were assayed for their ability
623 to bind synthetic biotinylated HBGAs A, B, Le^a, Le^b, Le^x, Le^y, H type 1, and H
624 type 3 by carbohydrate binding assay. Positive reactivity was defined as a value
625 greater or equal to 3X the background binding value.

626

627 **Table 2: GII.4 Mouse and Human mAb EIA Reactivity with Chronic Infection**
628 **Strains**

629 Mouse and human GII.4 monoclonal antibodies against were assayed for
630 reactivity with GII.4-2006b, P.D1, and P.D302 VLPs by multiple dilution EIA. The
631 mean percent binding (percent of the VLP bound to antibody in the dilution
632 course compared to the amount of VLP bound with antibody at 1 ug/mL) of each
633 VLP was fit with a sigmoidal curve, and the mean EC_{50} (µg/ml) EIA reactivity

titers for GII.4-2006b, P.D1, and P.D302 were calculated. * Mean EC_{50} EIA reactivity titer for the test VLP is significantly different from the mean EC_{50} for GII.4-2006b (light grey), or ** was significantly different from both GII.4-2006b and P.D1 ($p<0.05$) (dark grey). Monoclonal antibodies that did not demonstrate EIA reactivity at or above OD450 nm 0.2 at 1 ug/mL with a particular VLP are denoted by an EC_{50} of >1 ug/mL. Statistics were calculated by One-way ANOVA with Bonferroni post test.

Figure 2: GII.4 Mouse and Human mAb Blockade Response Against Chronic Infection Strains

(A-I) Mouse and human GII.4 monoclonal antibodies were assayed for ability to block GII.4-2006b, P.D1, and P.D302 VLP interaction with carbohydrate ligand. The mean percent control binding (percent of the VLP bound to carbohydrate ligand in the presence of an antibody compared to the amount of VLP bound with no antibody present) of each VLP was fit with a sigmoidal curve, and the mean EC_{50} (µg/ml) blockade titers for GII.4-2006b, P.D1, and P.D302 were calculated. Error bars represent 95% confidence intervals. * Mean EC_{50} blockade titer for the test VLP is significantly different from the mean EC_{50} for GII.4-2006b ($p<0.05$), or ** was significantly different from both GII.4-2006b and P.D1 ($p<0.05$). Monoclonal antibodies that did not block a particular VLP were assigned an EC_{50} of 2X the upper limit of detection for statistical analysis and are shown on the

graph by data points above the upper limit of detection (dashed line). Statistics were calculated by One-way ANOVA with Bonferroni post test.

Figure 3: Blockade Activity of Mouse Polyclonal Sera Against Homotypic and Heterotypic VLPs

Mice were immunized with VRP expressing the capsid gene of GII.4-2006b, GII.4-2009, P.D1, and P.D302, and sera collected from these mice were tested for blockade activity against GII.4-2006b, GII.4-2009, P.D1, and P.D302 VLPs. (A) Blockade activity of sera from mice immunized against GII.4-2006b (A), GII.4-2009 (B), P.D1 (C), and P.D302 (D) with homotypic and heterotypic VLPs. The mean percent control binding (percent of the VLP bound to carbohydrate ligand in the presence of sera compared to the amount of VLP bound with no sera present) of each VLP was fit with a sigmoidal curve, and the mean EC_{50} (% sera) blockade titers for GII.4-2006b, GII.4-2009, P.D1, and P.D302 were calculated. Error bars represent 95% confidence intervals. * Mean EC_{50} blockade titer for the test VLP is significantly different from the mean EC_{50} for the homotypic strain ($p<0.05$). Sera that did not block a particular VLP were assigned an EC_{50} of 10% sera for statistical analysis and are shown on the graph by data points above the upper limit of detection (dashed line). Statistics were calculated by One-way ANOVA with Bonferroni post test.

Figure 4: Antigenic Cartography for GII.4 Noroviruses

677 Multidimentional Scaling (MDS) was used to identify the antigenic relationships
678 between different norovirus strains. A) Euclidean antigenic distances between
679 virus strains were calculated based on the EC_{50} efficacy of antisera raised
680 against GII.4-1987, GII.4-2002, GII.4-2006b, GII.4-2009, P.D1 and P.D302 VLPs.
681 Green squares represent distances within either the early (1987, 1998 and 2002)
682 or late (2006, 2009 and 2012) virus groups. Purple squares show the distances
683 between early and late virus groups. (B-C) We determined XYZ-coordinates that
684 maintain the underlying Euclidean distances between viruses, while illustrating
685 the relationships between GII.4 norovirus strains, with each map-distance
686 roughly corresponding to a ~1.25-fold change in blockade response. B) Early
687 strains GII.4-1987 (yellow), GII.4-1997 (red), and GII.4-2002 (light blue) grouped
688 together (lower right hand group), and late strains GII.4-2006b (light purple),
689 GII.4-2009 (dark blue), and GII.4-2012 (dark purple) grouped together (lower left
690 hand group). P.D1 grouped with late strains, closest to GII.4-2006b, while
691 P.D302 was separate from either late or early strains (upper position). C) Side
692 view of the same 3D graph showing the antigenic differences between strains.

693

694 **Figure 5: Expansion of Epitope Site A**

695 Epitope A targeting human GII.4 mAb 43.9 was assayed for its ability to block
696 GII.4-2009 New Orleans, GII.4-2012 Sydney, GII.4-2012.09A, GII.4-2012.R373N,
697 and GII.4-2012.09A.R373N VLP interaction with carbohydrate ligand. The mean
698 percent control binding (percent of the VLP bound to carbohydrate ligand in the
699 presence of an antibody compared to the amount of VLP bound with no antibody

present) of each VLP was fit with a sigmoidal curve, and the mean EC_{50} (μg/ml) blockade titers for all VLPs were calculated. Error bars represent 95% confidence intervals. Statistics were calculated by One-way ANOVA with Dunnett's post test. * Mean EC_{50} blockade titer was significantly different from GII.4-2009.

Figure 6: Comparison of Epitope Site D Polar Interactions Among GII.4-2006 and Chronic Infection Strains

Pymol was used to model the polar interactions within residues 390-395 (A-C) and interactions between these residues and surrounding residues (D-F). GII.4-2006b is shown in purple (A and D), P.D1 is shown in teal (B and E), and P.D302 is shown in pink (C and F). Residues 390-395 are shown in orange for GII.4-2006b, yellow for P.D1, and aqua for P.D302. Dotted lines represent structure-based predicted polar interactions. Dark purple residues represent positions that interact with HBGAs (D-F).

References

1. Mattner F, Sohr D, Heim A, Gastmeier P, Vennema H, Koopmans M. 2006. Risk groups for clinical complications of norovirus infections: an outbreak investigation. Clin Microbiol Infect 12:69-74.
2. Murata T, Katsushima N, Mizuta K, Muraki Y, Hongo S, Matsuzaki Y. 2007. Prolonged norovirus shedding in infants <or=6 months of age with gastroenteritis. Pediatr Infect Dis J 26:46-49.
3. Okada M, Tanaka T, Oseto M, Takeda N, Shinozaki K. 2006. Genetic analysis of noroviruses associated with fatalities in healthcare facilities. Arch Virol 151:1635-1641.

4. Johnston CP, Qiu H, Ticehurst JR, Dickson C, Rosenbaum P, Lawson P, Stokes AB, Lowenstein CJ, Kaminsky M, Cosgrove SE, Green KY, Perl TM. 2007. Outbreak management and implications of a nosocomial norovirus outbreak. Clin Infect Dis 45:534-540.
5. Kroneman A, Vega E, Vennema H, Vinje J, White PA, Hansman G, Green K, Martella V, Katayama K, Koopmans M. 2013. Proposal for a unified norovirus nomenclature and genotyping. Arch Virol 158:2059-2068.
6. Prasad BV, Hardy ME, Dokland T, Bella J, Rossmann MG, Estes MK. 1999. X-ray crystallographic structure of the Norwalk virus capsid. Science 286:287-290.
7. Lindesmith LC, Donaldson EF, Lobue AD, Cannon JL, Zheng DP, Vinje J, Baric RS. 2008. Mechanisms of GII.4 norovirus persistence in human populations. PLoS Med 5:e31.
8. Donaldson EF, Lindesmith LC, Lobue AD, Baric RS. 2008. Norovirus pathogenesis: mechanisms of persistence and immune evasion in human populations. Immunol Rev 225:190-211.
9. Fankhauser RL, Monroe SS, Noel JS, Humphrey CD, Bresee JS, Parashar UD, Ando T, Glass RI. 2002. Epidemiologic and molecular trends of "Norwalk-like viruses" associated with outbreaks of gastroenteritis in the United States. J Infect Dis 186:1-7.
10. Siebenga JJ, Vennema H, Renckens B, de Bruin E, van der Veer B, Siezen RJ, Koopmans M. 2007. Epochal evolution of GGII.4 norovirus capsid proteins from 1995 to 2006. J Virol 81:9932-9941.
11. Allen DJ, Noad R, Samuel D, Gray JJ, Roy P, Iturriza-Gomara M. 2009. Characterisation of a GII-4 norovirus variant-specific surface-exposed site involved in antibody binding. Virol J 6:150.
12. Lindesmith LC, Donaldson EF, Baric RS. 2011. Norovirus GII.4 strain antigenic variation. J Virol 85:231-242.
13. Debbink K, Donaldson EF, Lindesmith LC, Baric RS. 2012. Genetic mapping of a highly variable norovirus GII.4 blockade epitope: potential role in escape from human herd immunity. J Virol 86:1214-1226.
14. Lindesmith LC, Beltramello M, Donaldson EF, Corti D, Swanstrom J, Debbink K, Lanzavecchia A, Baric RS. 2012. Immunogenetic mechanisms driving norovirus GII.4 antigenic variation. PLoS Pathog 8:e1002705.
15. Lindesmith LC, Debbink K, Swanstrom J, Vinje J, Costantini V, Baric RS, Donaldson EF. 2012. Monoclonal antibody-based antigenic mapping of norovirus GII.4-2002. J Virol 86:873-883.
16. Lindesmith LC, Costantini V, Swanstrom J, Debbink K, Donaldson EF, Vinje J, Baric RS. 2013. Emergence of a norovirus GII.4 strain correlates with changes in evolving blockade epitopes. J Virol 87:2803-2813.
17. Debbink K, Lindesmith LC, Donaldson EF, Costantini V, Beltramello M, Corti D, Swanstrom J, Lanzavecchia A, Vinje J, Baric RS. 2013. Emergence of New Pandemic GII.4 Sydney Norovirus Strain Correlates with Escape from Herd Immunity. J Infect Dis.

18. Rockx B, De Wit M, Vennema H, Vinje J, De Bruin E, Van Duynhoven Y, Koopmans M. 2002. Natural history of human calicivirus infection: a prospective cohort study. Clin Infect Dis 35:246-253.
19. Obara M, Hasegawa S, Iwai M, Horimoto E, Nakamura K, Kurata T, Saito N, Oe H, Takizawa T. 2008. Single base substitutions in the capsid region of the norovirus genome during viral shedding in cases of infection in areas where norovirus infection is endemic. J Clin Microbiol 46:3397-3403.
20. Siebenga J, Kroneman A, Vennema H, Duizer E, Koopmans M. 2008. Food-borne viruses in Europe network report: the norovirus GII.4 2006b (for US named Minerva-like, for Japan Kobe034-like, for UK V6) variant now dominant in early seasonal surveillance. Euro Surveill 13.
21. Nilsson M, Hedlund KO, Thorhagen M, Larson G, Johansen K, Ekspong A, Svensson L. 2003. Evolution of human calicivirus RNA in vivo: accumulation of mutations in the protruding P2 domain of the capsid leads to structural changes and possibly a new phenotype. J Virol 77:13117-13124.
22. Schorn R, Hohne M, Meerbach A, Bossart W, Wuthrich RP, Schreier E, Muller NJ, Fehr T. 2010. Chronic norovirus infection after kidney transplantation: molecular evidence for immune-driven viral evolution. Clin Infect Dis 51:307-314.
23. Hoffmann D, Hutzenthaler M, Seebach J, Panning M, Umgelter A, Menzel H, Protzer U, Metzler D. 2012. Norovirus GII.4 and GII.7 capsid sequences undergo positive selection in chronically infected patients. Infect Genet Evol 12:461-466.
24. Ludwig A, Adams O, Laws HJ, Schroten H, Tenenbaum T. 2008. Quantitative detection of norovirus excretion in pediatric patients with cancer and prolonged gastroenteritis and shedding of norovirus. J Med Virol 80:1461-1467.
25. Bull RA, Eden JS, Luciani F, McElroy K, Rawlinson WD, White PA. 2012. Contribution of intra- and interhost dynamics to norovirus evolution. J Virol 86:3219-3229.
26. Koo HL, DuPont HL. 2009. Noroviruses as a potential cause of protracted and lethal disease in immunocompromised patients. Clin Infect Dis 49:1069-1071.
27. Capizzi T, Makari-Judson G, Steingart R, Mertens WC. 2011. Chronic diarrhea associated with persistent norovirus excretion in patients with chronic lymphocytic leukemia: report of two cases. BMC Infect Dis 11:131.
28. Boillat Blanco N, Kuonen R, Bellini C, Manuel O, Estrade C, Mazza-Stalder J, Aubert JD, Sahli R, Meylan P. 2011. Chronic norovirus gastroenteritis in a double hematopoietic stem cell and lung transplant recipient. Transpl Infect Dis 13:213-215.
29. Florescu DF, Hill LA, McCartan MA, Grant W. 2008. Two cases of Norwalk virus enteritis following small bowel transplantation treated with oral human serum immunoglobulin. Pediatr Transplant 12:372-375.
30. Florescu DF, Hermsen ED, Kwon JY, Gumeel D, Grant WJ, Mercer DF, Kalil AC. 2011. Is there a role for oral human immunoglobulin in the treatment for

816 norovirus enteritis in immunocompromised patients? Pediatr Transplant
817 15:718-721.
818 31. Ebdrup L, Bottiger B, Molgaard H, Laursen AL. 2011. Devastating diarrhoea in
819 a heart-transplanted patient. J Clin Virol 50:263-265.
820 32. Chagla Z, Quirt J, Woodward K, Neary J, Rutherford C. 2013. Chronic
821 norovirus infection in a transplant patient successfully treated with enterally
822 administered immune globulin. J Clin Virol.
823 33. Sukhrie FH, Siebenga JJ, Beersma MF, Koopmans M. 2010. Chronic shedders
824 as reservoir for nosocomial transmission of norovirus. J Clin Microbiol
825 48:4303-4305.
826 34. Kaufman SS, Chatterjee NK, Fuschino ME, Morse DL, Morotti RA, Magid MS,
827 Gondolesi GE, Florman SS, Fishbein TM. 2005. Characteristics of human
828 calicivirus enteritis in intestinal transplant recipients. J Pediatr Gastroenterol
829 Nutr 40:328-333.
830 35. Siebenga JJ, Beersma MF, Vennema H, van Biezen P, Hartwig NJ, Koopmans M.
831 2008. High prevalence of prolonged norovirus shedding and illness among
832 hospitalized patients: a model for in vivo molecular evolution. J Infect Dis
833 198:994-1001.
834 36. Eden JS, Tanaka MM, Boni MF, Rawlinson WD, White PA. 2013.
835 Recombination within the pandemic norovirus GII.4 lineage. J Virol 87:6270-
836 6282.
837 37. Cao S, Lou Z, Tan M, Chen Y, Liu Y, Zhang Z, Zhang XC, Jiang X, Li X, Rao Z.
838 2007. Structural basis for the recognition of blood group trisaccharides by
839 norovirus. J Virol 81:5949-5957.
840 38. Baric RS, Yount B, Lindesmith L, Harrington PR, Greene SR, Tseng FC, Davis
841 N, Johnston RE, Klapper DG, Moe CL. 2002. Expression and self-assembly of
842 norwalk virus capsid protein from venezuelan equine encephalitis virus
843 replicons. J Virol 76:3023-3030.
844 39. Barnett JL, Yang J, Cai Z, Zhang T, Wan XF. 2012. AntigenMap 3D: an online
845 antigenic cartography resource. Bioinformatics 28:1292-1293.
846 40. Cai Z, Zhang T, Wan XF. 2010. A computational framework for influenza
847 antigenic cartography. PLoS Comput Biol 6:e1000949.
848 41. Cannon JL, Lindesmith LC, Donaldson EF, Saxe L, Baric RS, Vinje J. 2009. Herd
849 immunity to GII.4 noroviruses is supported by outbreak patient sera. J Virol
850 83:5363-5374.
851 42. Reeck A, Kavanagh O, Estes MK, Opekun AR, Gilger MA, Graham DY, Atmar
852 RL. 2010. Serological correlate of protection against norovirus-induced
853 gastroenteritis. J Infect Dis 202:1212-1218.
854 43. Allen DJ, Adams NL, Aladin F, Harris JP, Brown DW. 2014. Emergence of the
855 GII-4 Norovirus Sydney2012 Strain in England, Winter 2012-2013. PLoS One
856 9:e88978.
857 44. Roddie C, Paul JP, Benjamin R, Gallimore CI, Xerry J, Gray JJ, Peggs KS, Morris
858 EC, Thomson KJ, Ward KN. 2009. Allogeneic hematopoietic stem cell
859 transplantation and norovirus gastroenteritis: a previously unrecognized
860 cause of morbidity. Clin Infect Dis 49:1061-1068.

45. Glass RI, Parashar UD, Estes MK. 2009. Norovirus gastroenteritis. N Engl J Med 361:1776-1785.
46. Atmar RL, Opekun AR, Gilger MA, Estes MK, Crawford SE, Neill FH, Graham DY. 2008. Norwalk virus shedding after experimental human infection. Emerg Infect Dis 14:1553-1557.
47. Etherington GJ, Ring SM, Charleston MA, Dicks J, Rayward-Smith VJ, Roberts IN. 2006. Tracing the origin and co-phylogeny of the caliciviruses. J Gen Virol 87:1229-1235.
48. Tan M, Xia M, Cao S, Huang P, Farkas T, Meller J, Hegde RS, Li X, Rao Z, Jiang X. 2008. Elucidation of strain-specific interaction of a GII-4 norovirus with HBGA receptors by site-directed mutagenesis study. Virology 379:324-334.
49. Bedford T, Suchard MA, Lemey P, Dudas G, Gregory V, Hay AJ, McCauley JW, Russell CA, Smith DJ, Rambaut A. 2014. Integrating influenza antigenic dynamics with molecular evolution. Elife 3:e01914.

	A	B	Le^a	Le^b	Le^x	Le^y	H type 1	H type 3
GII.4-2006	+	+	-	+	-	+	-	+
P.D1	+	+	-	-	-	-	-	+
P.D302	-	+	-	-	-	-	-	+

Table 1: Chronic Infection Strain HBGA Binding Preferences
VLPs representing GII.4-2006b, P.D1, and P.D302 were assayed for their ability to bind synthetic biotinylated HBGAs A, B, Le^a, Le^b, Le^x, Le^y, H type 1, and H type 3 by carbohydrate binding assay. Positive reactivity was defined as a value greater or equal to 3X the background binding value.

mAb	Epitope Targeted	Mean EC_{50} (Upper/Lower Limit)		
		GII.4-2006	P.D1	P.D302
GII.4-2006-G2	A	0.113 (0.130/0.098)	0.290* (0.357/0.235)	>1.00**
GII.4-2006-G3	A	0.097 (0.110/0.085)	0.127 (0.156/0.104)	>1.00**
GII.4-2006-G4	A	0.011 (0.013/0.008)	0.028* (0.045/0.017)	>1.00**
GII.4-2006-G6	A	0.024 (0.029/0.021)	0.052* (0.067/0.040)	0.201** (0.232/0.175)
GII.4-2006-G7	A	0.021 (0.026/0.017)	0.02 (0.027/0.015)	>1.00**
NVB43.9	A	0.024 (0.026/0.022)	0.046* (0.051/0.041)	>1.00**
NVB111	A	0.147 (0.211/0.103)	>1.00*	>1.00*
NVB97	D	0.082 (0.131/0.052)	0.059 (0.084/0.041)	>1.00**
NVB71.4	conserved GII.4	0.151 (0.182/0.125)	0.129 (0.176/0.095)	0.13 (0.168/0.101)

Table 2: GII.4 Mouse and Human mAb EIA Reactivity with Chronic Infection Strains
Mouse and human GII.4 monoclonal antibodies against were assayed for reactivity with GII.4-2006b, P.D1, and P.D302 VLPs by multiple dilution EIA. The mean percent binding (percent of the VLP bound to antibody in the dilution course compared to the amount of VLP bound with antibody at 1 ug/mL) of each VLP was fit with a sigmoidal curve, and the mean EC_{50} (µg/ml) EIA reactivity titers for GII.4-2006b, P.D1, and P.D302 were calculated. * Mean EC_{50} EIA reactivity titer for the test VLP is significantly different from the mean EC_{50} for GII.4-2006b (light grey), or ** was significantly different from both GII.4-2006b and P.D1 ($p<0.05$) (dark grey). Monoclonal antibodies that did not demonstrate EIA reactivity at or above OD450 nm 0.2 at 1 ug/mL with a particular VLP are denoted by an EC_{50} of >1 ug/mL. Statistics were calculated by One-way ANOVA with Bonferroni post test.

A

	248	255	271	292	294	295	296	329	340	348	352	356	368	373	391	393	404	412	414	425	426	434
GII.4-2006	K	G	V	H	A	G	S	K	G	K	Y	A	S	N	D	S	V	N	H	T	F	F
P.D1	R	S	M	H	A	G	S	K	G	K	Y	A	A	N	D	G	A	N	Q	N	S	F
P.D302	R	S	M	Q	G	S	T	R	R	T	S	V	A	H	N	S	V	D	Q	N	S	S

B

	A								D				E			
	292	294	295	296	297	298	368	372	373	391	393	394	395	404	407	412	414
GII.4-2006	H	A	G	S	R	N	S	E	N	D	S	T	T	V	S	N	H
P.D1	H	A	G	S	R	N	A	E	N	D	G	T	T	A	S	N	Q
P.D302	Q	G	S	T	R	N	A	E	H	N	S	T	T	V	S	D	Q

C

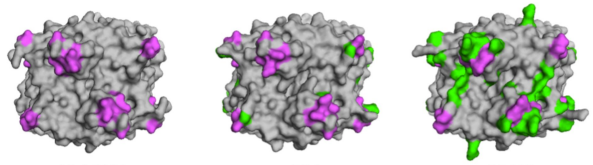

GII.4-2006
Parental Strain

P.D1
Day 1 of monitoring

P.D302
Day 302 of monitoring

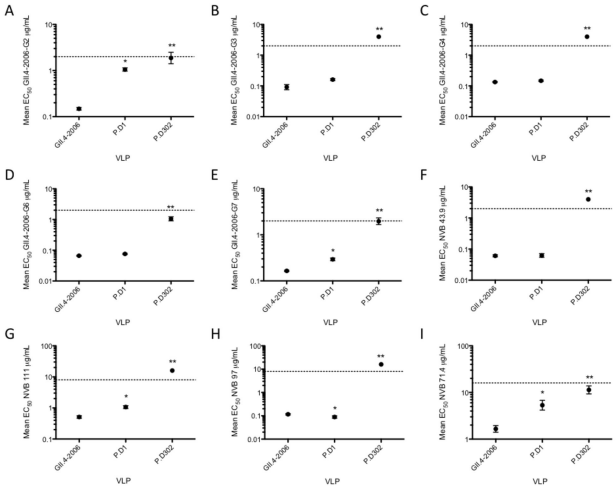

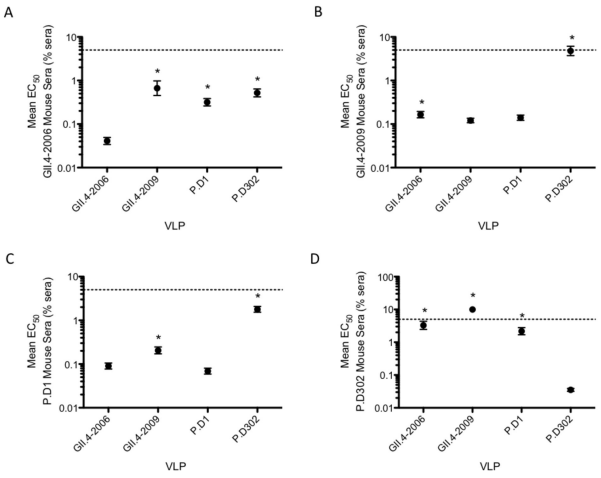

A

Antigenic Distances Between Viruses

Virus Isolate	1997	2002	2006	2009	2012	P.D1	P.D302
1987	2.11	3.34	12.21	10.07	8.64	11.18	10.34
1997		3.53	13.32	11.39	10.14	12.38	11.62
2002			12.11	9.94	8.49	11.06	10.22
2006				4.26	6.39	3.04	9.91
2009					3.14	2.26	9.44
2012						5.09	8.73
P.D1							9.15

B

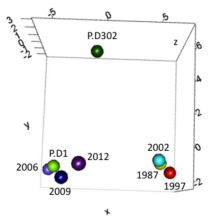

C